DOI: 10.1002/chem.200700628

Ferromagnetic Coupling in Trinuclear, Partial Cubane Cu^{II} Complexes with a μ_3-OH Core: Magnetostructural Correlations

Biswarup Sarkar,[a] Mau Sinha Ray,[a] Yi-Zhi Li,[b] You Song,[b] Albert Figuerola,*[c] Eliseo Ruiz,[d] Jordi Cirera,[d] Joan Cano,[d, e] and Ashutosh Ghosh*[a]

Abstract: Three new trinuclear copper(II) complexes, $[(CuL^1)_3(\mu_3\text{-}OH)][ClO_4]_2\cdot 3H_2O$ (**1**), $[(CuL^2)_3(\mu_3\text{-}OH)][ClO_4]_2\cdot H_2O$ (**2**), and $[(CuL^3)_3(\mu_3\text{-}OH)][ClO_4]_2\cdot 7H_2O$ (**3**) have been synthesized from the three tridentate Schiff bases HL^1, HL^2, and HL^3 (HL^1 = 6-aminomethyl-3-methyl-1-phenyl-4-azahex-2-en-1-one, HL^2 = 6-aminoethyl-3-methyl-1-phenyl-4-azahex-2-en-1-one, and HL^3 = 6-aminodimethyl-3-methyl-1-phenyl-4-azahex-2-en-1-one). They have been characterized by X-ray crystallography and IR and UV spectroscopy, and their magnetic properties have been investigated. All the compounds contain a partial cubane $[Cu_3O_4]$ core consisting of the trinuclear unit $[(CuL)_3(\mu_3\text{-}OH)]^{2+}$, perchlorate ions, and water molecules. In each of the complexes, the copper atoms are five-coordinate with a distorted square-pyramidal geometry except complex **1**, in which one of the Cu^{II} of the trinuclear unit is weakly coordinated to one of the perchlorate ions. Magnetic measurements performed in SQUID MPMS-XL7 using polycrystalline samples at an applied field of 2 kOe indicate a global intramolecular ferromagnetic coupling. Magnetostructural correlations have been calculated on the basis of theoretical models without symmetry restriction. Continuous shape measurements are an appropriate tool for establishing the degree of distortion of the Cu^{II} from square-planar geometry. Structural, theoretical, and experimental magnetic data indicate that the higher the degree of distortion, the greater the ferromagnetic coupling.

Keywords: copper · magnetic properties · Schiff bases · structure elucidation · tridentate ligands

Introduction

Magnetic exchange in simple polynuclear paramagnetic clusters is a current focus of study in magnetochemistry.[1] It is particularly important to find well-characterized compounds for which precise information can be obtained on both the ground state and the excited states of a strongly coupled paramagnetic system. The magnetic exchange model can be tested in cyclic trinuclear complexes of the $[Cu_3O]$ core, a simple three-electron spin system. The three unpaired electrons on this core interact magnetically through superexchange involving Cu^{II}-O-Cu^{II} pathways. The core could exist in either a spin-frustrated ($S_{total} = {}^1/_2$, doubly degenerate) state or in a $S_{total} = {}^3/_2$ quartet state resulting in the antiferro- and ferromagnetic complexes, respectively. Magnetostructural correlation in the hydroxide-, alkoxide-, or phenoxide-bridged complexes show that the major factors controlling spin coupling between the metal centers are the Cu-O-Cu bridging angles and the out-of-plane angle of the substituents of the bridging oxygens.[2] To our knowledge, ten copper(II) compounds with a partial cubane $[Cu_3O_4]$ core and an NNO donor Schiff base as peripheral bridges have been

[a] B. Sarkar, Dr. M. S. Ray, Dr. A. Ghosh
Department of Chemistry, University College of Science
University of Calcutta, 92 A.P.C. Road, Kolkata-700009 (India)
Fax: (+91) 33-2351-9755
E-mail: ghosh_59@yahoo.com

[b] Dr. Y.-Z. Li, Dr. Y. Song
Coordination Chemistry Institute and
the State Key Laboratory of Coordination Chemistry
Nanjing University, Nanjing 210093 (Republic of China)

[c] Dr. A. Figuerola
Department de Química Inorgànica and
Institut de Nanociència i Nanotecnologia
Universitat de Barcelona, Av. Diagonal 647, 08028 Barcelona (Spain)
Fax: (34)934907725
E-mail: albert.figuerola@qi.ub.es

[d] Dr. E. Ruiz, Dr. J. Cirera, Dr. J. Cano
Department de Química Inorgànica,
Centre de Recerca en Química Teòrica (CERQT)
and Institut de Nanociència i Nanotecnologia
Universitat de Barcelona, Av. Diagonal 647, 08028 Barcelona (Spain)

[e] Dr. J. Cano
Institució Catalana de Recerca i Estudis Avançats (ICREA)
Passeig Lluís Companys 27, 08010 Barcelona (Spain)

Supporting information for this article is available on the WWW under http://www.chemeurj.org/ or from the author.

characterized structurally and magnetically to date.[3–7] The Schiff bases were derived from acetylacetone in seven compounds,[3–6] 1-benzoylacetone in two compounds,[7] and salicylaldehyde in one compound.[5] All the complexes except that derived from salicylaldehyde[5] are coupled antiferromagnetically. For the magnetostructural correlations of the acetylacetone-derived complexes, the greatest coplanarity of the three principal ligand planes, the shortest distance of the O(H) above the Cu_3 plane, and the greatest Cu-O-Cu′ angles appear to provide the strongest antiferromagnetic coupling. We have tested the validity of this relationship in other systems also.

In this paper we report the synthesis, crystal structure, and magnetic properties of three new cyclic trinuclear μ_3-hydroxo-bridged copper(II) compounds, $[(CuL)_3(OH)][ClO_4]_2 \cdot n H_2O$, in which L is a Schiff base derived from three different diamines and 1-benzoylacetone (ligands L^1, L^2, and L^3 in Scheme 1; HL^1 = 6-aminomethyl-3-methyl-1-phenyl-4-azahex-2-en-1-one, HL^2 = 6-aminoethyl-3-methyl-1-phenyl-4-azahex-2-en-1-one, and HL^3 = 6-aminodimethyl-3-methyl-1-phenyl-4-azahex-2-en-1-one). All three complexes exhibit weak ferromagnetic exchange interactions. New magnetostructural correlations for these compounds have been proposed on the basis of calculations and continuous shape measurements.

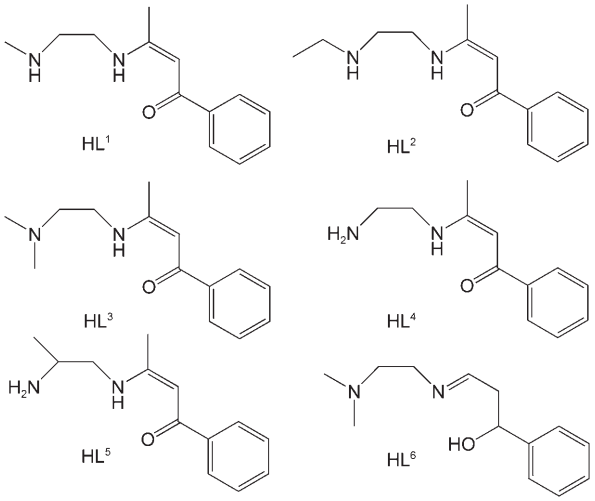

Scheme 1. Chemical structure of aromatic Schiff base peripheral ligands used in the synthesis of $[Cu_3O_4]$-type compounds **1**–**6**.

Results and Discussion

Upon treatment with a mixture of methanol/copper perchlorate hexahydrate/triethylamine (1:1:1), the tridentate ligands HL^1, HL^2, and HL^3 (Scheme 1) yielded the trinuclear complexes **1**, **2**, and **3** respectively. Complexes **1** and **3** were obtained readily on mixing the constituents; no hydrolysis of the product occurred during synthesis. The ligand HL^2 is rather susceptible to hydrolysis, however, and dry methanol was used as the reaction medium for higher yields of **2**. All the complexes can be purified easily by recrystallization from methanol.

IR and electronic spectra: In all three complexes the presence of a broad band at 3510 (**1**), 3502 (**2**), and 3528 cm^{-1} (**3**) is assigned to ν(OH) of the triply bridging hydroxy group. The peak positions corroborate well the strength of the H bond involving the hydroxyl group. The X-ray analysis shows that the H bond is the strongest in **2** and weakest in **3** (see crystal structure, below). This is substantiated by the appearance of this band at the lowest and highest wavenumbers, respectively. There is another broad band at 3400 (**1**), 3440 (**2**), and 3450 cm^{-1} (**3**), due to the presence of lattice water molecules. The sharp peaks at 3249 and 3270 cm^{-1} for complexes **1** and **2** indicate the presence of an N–H group. The IR spectrum of complex **3** does not show a band in this region, corroborating the absence of an N–H group in HL^3. The other characteristic bands are easily located at 1592, 1600, and 1610 cm^{-1} (ν(C=O), ν(C=C)), and 1515, 1520, and 1518 cm^{-1} (ν(C=N)) for complexes **1**, **2**, and **3** respectively. There is a broad band at 1105 (**1**), 1100 (**2**), and 1095 cm^{-1} (**3**), due to the ν_3 mode of perchlorate anions in T_d symmetry.

The electronic spectra in acetonitrile as well as in nujol mull of the three complexes display a single absorption band at 591 (**1**), 587 (**2**), and 581 nm (**3**). These spectra are typical of square-based geometry around the copper centers.[8]

Crystal structures: Crystals of complexes **1**, **2**, and **3** belong to the triclinic, orthorombic, and monoclinic crystal systems with $P\bar{1}$, *Pbca*, and $P2_1/c$ space groups respectively. Crystallographic data for **1**–**3** are listed in Table 1. However, the molecular units for all three complexes show similar characteristics. The structures of the three complexes consist of dipositive trinuclear cations $[(CuL)_3(\mu_3\text{-}OH)]^{2+}$ having a partial cubane core and two noncoordinated perchlorate anions required to balance the charge. In addition, there are lattice water molecules in all three complexes. The trinuclear $[(CuL^1)_3(\mu_3\text{-}OH)]^{2+}$ ion of complex **1** is shown in perspective (Figure 1); complexes **2** and **3** have similar molecular structure (Figures S1 and S2 respectively, Supporting Information). The trinuclear cations of each complex comprise three [CuL] subunits (in which L represents the deprotonated tridentate monoanionic ligand), which are roughly perpendicular to each other and are interconnected through two types of oxygen bridges afforded by the carbonyl oxygen atoms of the ligands and the central OH^- group. The presence of the OH^- group has been confirmed by the location of the hydrogen atom at the expected position in the final difference Fourier map, by the electroneutrality of the crystal, and by the trigonal pyramid structure formed by the Cu_3O fragment, in which the oxygen is located at the apex of the pyramid and the three copper atoms are at the corners of an approximately equilateral triangle.

Table 1. Crystallographic data and structural refinement of complexes **1**, **2**, and **3**.

	1	**2**	**3**
formula	$C_{39}H_{58}N_6O_{15}Cu_3Cl_2$	$C_{42}H_{60}N_6O_{13}Cu_3Cl_2$	$C_{42}H_{72}N_6O_{19}Cu_3Cl_2$
M_r	1112.43	1118.48	1226.53
T [K]	293	293	293
space group	$P\bar{1}$	*Pbca*	*P*21/*c*
crystal system	triclinic	orthorhombic	monoclinic
a [Å]	13.236(3)	16.639(3)	13.599(2)
b [Å]	13.319(3)	14.566(3)	35.869(5)
c [Å]	15.601(3)	41.226(8)	13.916(2)
α [°]	94.95(3)	90	90
β [°]	100.23(3)	90	114.502(3)
γ [°]	113.69(3)	90	90
V [Å^3]	2440.3(8)	9992(3)	6176.5(16)
Z	2	8	4
ρ_{calcd} [gm cm^{-3}]	1.514	1.487	1.261
μ [mm^{-1}]	1.474	1.438	1.169
F(000)	1150	4632	2436
R indices [$I>2\sigma(I)$]	$R_1=0.0604$	$R_1=0.0631$	$R_1=0.0573$
	$wR_2=0.1288$	$wR_2=0.1531$	$wR_2=0.1323$

case lacks any element of threefold symmetry. The Cu–O and Cu–N distances are comparable with those reported for the analogous systems.[3–7,9] The square-pyramidal geometry within each subunit is distorted in the usual way: that is, the copper ion is displaced from the basal plane toward the apical oxygen by 0.136(1), 0.168(1), and 0.165(1) Å for Cu1; 0.078(1), 0.134(1), and 0.153(1) Å for Cu2; and 0.136(1), 0.131(1), and 0.147(1) Å for Cu3 in complexes **1**, **2**, and **3**, respectively. The Addison parameter (τ),[10]

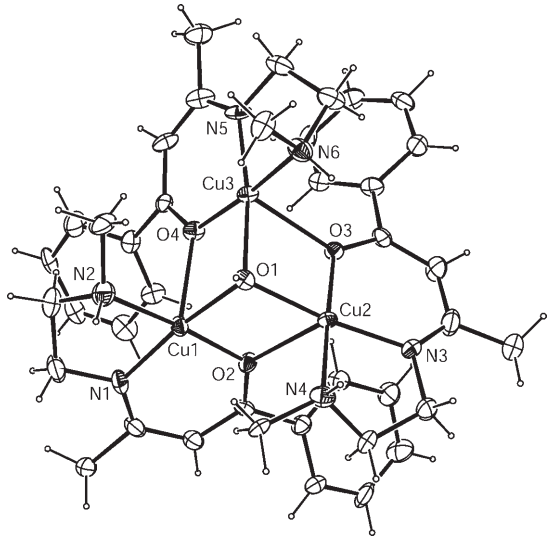

Figure 1. ORTEP-3 view of the $[(CuL^1)_3(OH)]^{2+}$ cation of complex **1** (30% thermal ellipsoids) including the atom numbering scheme.

Table 2. Selected bond lengths [Å] of complexes **1**, **2**, and **3**.

	1	**2**	**3**
Cu1–O1	1.975(3)	2.003(3)	2.039(2)
Cu1–O2	1.915(3)	1.924(3)	1.932(3)
Cu1–O4	2.367(3)	2.313(3)	2.366(2)
Cu1–N1	1.946(3)	1.949(5)	1.942(4)
Cu1–N2	2.021(4)	1.988(5)	2.052(4)
Cu2–O1	2.000(3)	2.016(3)	2.033(3)
Cu2–O2	2.440(3)	2.376(3)	2.311(3)
Cu2–O3	1.899(3)	1.925(3)	1.931(3)
Cu2–N3	1.928(4)	1.927(5)	1.929(4)
Cu2–N4	2.041(4)	2.054(5)	2.027(4)
Cu3–O1	2.015(3)	2.010(3)	2.035(2)
Cu3–O3	2.354(3)	2.332(3)	2.309(3)
Cu3–O4	1.893(3)	1.911(3)	1.913(3)
Cu3–N5	1.947(4)	1.940(4)	1.936(4)
Cu3–N6	2.008(3)	2.030(4)	2.033(4)

Selected bond lengths and angles for complexes **1–3** are listed in Tables 2 and 3. The geometry at each copper(II) ion is best described as a distorted (4+1) (NNOO+O) square-based pyramid except in complex **1**, in which one of the copper ions (Cu2–O5 = 2.776(3) Å) is weakly coordinated to a perchlorate ion to form an elongated distorted octahedron. The basal plane around the copper atom in each [CuL] subunit for each trinuclear cation consists of two nitrogen atoms (one imine and one amino) and one carbonyl oxygen atom from L and the hydroxy oxygen atom, while the carbonyl oxygen atom of a second ligand occupies the apical position. Thus each carbonyl oxygen atom within the basal plane of one [CuL] subunit is in turn apical to a copper atom in another subunit (Figure 1 and Figures S1 and S2). As expected, the axial Cu–O bonds are longer than the equatorial ones (Table 2). The overall structure in each

which is an index of distortion from the square-pyramidal to the trigonal-bipyramidal geometry, is calculated to be 0.08, 0.005, and 0.08 for Cu1, 0.09, 0.04, and 0.06 for Cu2, and 0.05, 0.11, and 0.02 for Cu3 in complexes **1**, **2**, and **3** respectively.

The six-membered chelate ring formed by the benzoylacetone moiety is essentially planar and the interatomic distances and angles of the ring are roughly identical in the three mononuclear units of all three complexes, except that in **3** the ring in the Cu2 subunit deviates considerably from planarity. This six-membered ring assumes almost a boat conformation with puckering parameters $\varphi = 129(3)°$, $\theta = 122.4(26)°$, and $Q = 0.087(4)$ Å.[11] The five-membered chelate ring within each subunit incorporating the dimethylene fragments from the starting diamines shows different conformations in all three complexes. For **1**, the five-membered chelate ring in all three subunits assumes a half-chair conformation. In **2** this ring with Cu1 is envelope on N2,[11] whereas with Cu2 and Cu3 it has a half-chair conformation. In complex **3**, it assumes a half-chair conformation in both the

Table 3. Selected bond angles [°] of complexes **1**, **2**, and **3**.

	1	2	3
O1-Cu1-O2	85.2(1)	85.6(1)	83.8(1)
O1-Cu1-O4	73.8(1)	73.3(1)	73.3(1)
O1-Cu1-N1	169.7(1)	170.3(2)	168.1(1)
O1-Cu1-N2	95.9(2)	94.1(2)	96.6(1)
O2-Cu1-O4	92.6(1)	93.7(1)	92.1(1)
O2-Cu1-N1	93.8(1)	93.1(2)	93.6(1)
O2-Cu1-N2	174.7(2)	170.1(2)	172.7(1)
O4-Cu1-N1	116.4(1)	116.4(2)	118.4(1)
O4-Cu1-N2	92.7(1)	95.7(2)	94.9(1)
N1-Cu1-N2	84.2(2)	85.6(2)	84.6(2)
O1-Cu2-O2	71.9(1)	74.3(1)	74.9(1)
O1-Cu2-O3	83.9(1)	83.9(1)	84.0(1)
O1-Cu2-N3	172.3(1)	171.0(2)	169.0(1)
O1-Cu2-N4	96.8(1)	94.9(2)	96.1(1)
O2-Cu2-O3	89.5(1)	91.3(1)	91.7(1)
O2-Cu2-N3	115.4(1)	114.5(2)	115.6(1)
O2-Cu2-N4	92.5(1)	94.5(2)	95.4(1)
O3-Cu2-N3	93.6(1)	93.8(2)	92.4(1)
O3-Cu2-N4	177.9(1)	173.6(2)	172.6(1)
N3-Cu2-N4	85.5(2)	86.3(2)	86.1(2)
O1-Cu3-O3	72.9(1)	74.3(1)	75.0(1)
O1-Cu3-O4	84.5(1)	82.6(1)	83.9(1)
O1-Cu3-N5	171.0(1)	169.2(2)	170.6(2)
O1-Cu3-N6	95.63(14)	96.5(2)	97.1(1)
O3-Cu3-O4	94.4(1)	90.6(1)	93.8(1)
O3-Cu3-N5	116.1(1)	116.2(2)	114.3(1)
O3-Cu3-N6	91.4(1)	94.4(2)	94.1(1)
O4-Cu3-N5	93.6(1)	94.2(2)	93.6(1)
O4-Cu3-N6	173.9(2)	175.5(2)	172.1(2)
N5-Cu3-N6	85.4(1)	85.9(2)	84.0(2)
Cu1-O1-Cu2	107.3(1)	104.6(1)	103.1(1)
Cu1-O1-Cu3	105.3(1)	105.5(1)	104.9(1)
Cu2-O1-Cu3	105.1(1)	104.1(1)	103.1(1)

Cu1 and the Cu2 subunits, whereas with Cu3 it is envelope on N6.[11]

Except for the weak interaction between Cu2 and O5 in complex **1**, the perchlorate anions are noncoordinating in all the complexes. All the other oxygen atoms of the perchlorate anions lie more than 3 Å from the copper centers. The perchlorate anions are involved in hydrogen bonding in all three complexes.

In complex **1** the two centrosymmetrically related trimers are linked through lattice water molecules and noncoordinating perchlorate anions by both N–H···O and O–H···O contacts. A view of the resulting centrosymmetric dimeric superstructure of **1** is shown in Figure 2. All three terminal amine hydrogen atoms in the molecule as well as the hydroxo H atom are involved in the hydrogen-bonding network (Table 4). Among them, the H atoms H6(N6) and H4(N4) are involved in bifurcated hydrogen bonding with a pair of centrosymmetrically related perchlorate ions (Figure 2, Table 4). The hydrogen atom H1 of the triply bridging hydroxo group is involved in a strong N–H···O bond with the oxygen atom O15 of one water molecule. The two hydrogen atoms H15c and H15d of this water molecule form O–H···O contacts with the oxygen atoms O13′ and O8′ of the symmetry-related water molecule and perchlorate ion respectively. H14c and H13a of other two water molecules

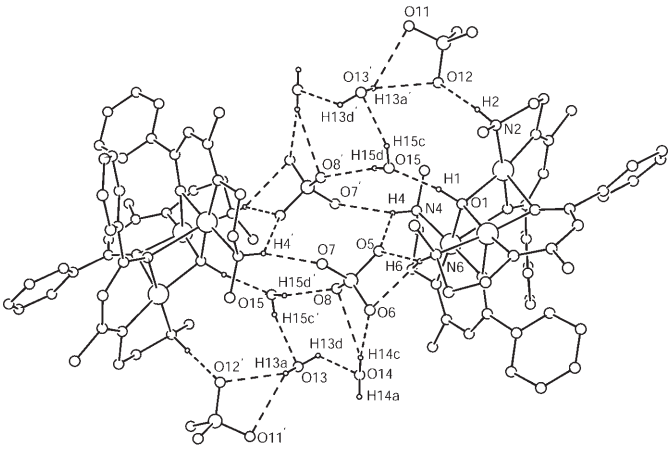

Figure 2. Aggregation of isolated trimeric units by hydrogen bonding interactions between the $[(CuL^1)_3(OH)]^{2+}$ ion and perchlorate anions in the solid state of complex **1**. Atoms marked with a prime are transformed by symmetry element $1-x, 2-y, 1-z$.

Table 4. Hydrogen bonding distances and angles for complexes **1**–**3**.

	D–H···A	D–H [Å]	D–A [Å]	H–A [Å]	D–H–A [°]
1	N6–H6···O5	0.910	3.150(6)	2.292	156.9
	N6–H6···O6	0.910	3.340(6)	2.545	146.3
	N4–H4···O5	0.909	3.045(5)	2.486	120.0
	N2–H2···O12	0.909	3.123(6)	2.246	161.8
	O1–H1···O15	0.981	2.834(4)	1.865	169.3
	O13–H13d···O14	0.851	2.666(8)	2.059	127.8
	O14–H14c···O6	0.849	3.343(7)	2.499	172.4
	O14–H14c···O8	0.849	3.187(7)	2.546	133.0
	N4–H4···O7[a]	0.909	3.079(6)	2.430	128.4
	O13–H13a···O11[a]	0.849	3.165(7)	2.582	126.9
	O13–H13a···O12[a]	0.849	3.174(6)	2.459	142.2
	O15–H15c···O13[a]	0.851	2.759(6)	2.112	132.5
	O15–H15d···O8[a]	0.849	3.122(6)	2.317	158.4
2	N2–H2a···O11	0.911	3.213(6)	2.312	170.0
	N4–H4a···O5	0.911	3.002(6)	2.096	172.9
	N6–H6a···O12	0.910	3.152(7)	2.299	155.7
	O1–H1a···O13	0.980	2.796(19)	1.817	178.5
	O13–H13f···O9	0.849	2.736(15)	1.887	179.5
3	O1–H1···O6	0.980	2.922(4)	1.946	173.9
	O17–H17d···O16	0.849	2.879(7)	2.088	154.5
	O18–H18d···O16	0.850	3.055(4)	2.210	180.0

[a] Symmetry code: $1-x, 2-y, 1-z$

are involved in bifurcated O–H···O contacts with O6 and O8 of a perchlorate ion and O11′ and O12′ of the symmetry-related perchlorate ion. These two water molecules (O13 and O14) are also interconnected through H13d. In complexes **2** and **3** trinuclear units are not linked each other by H bonds. In **2** oxygen atoms of perchlorate ions (O5 of one and O11 and O12 of another) are involved in N–H···O contacts with the amine hydrogen atoms (Figure S3, Table 4). The lattice water molecule forms strong O–H···O hydrogen bonds with H1 of the triply bridging hydroxo group and O9 of one perchlorate ion. In complex **3** all the amine hydrogen atoms are methyl-substituted. Only one intramolecular O–H···O contact between H1 of the triply bridging hydroxo

group and O6 of one perchlorate anion is observed (Figure S4, Table 4)

Magnetic properties: The variable-temperature susceptibilities for complexes **1**, **2**, and **3** were measured over the range 2–300 K with an applied magnetic field of 0.2 T. The temperature dependence of $\chi_M T$ on T (χ_M = magnetic susceptibility per $[Cu_3O_4]$ entity) for the three complexes is shown in Figure 3. At room temperature, the $\chi_M T$ values (1.27 (**1**), 1.16 (**2**), and 1.17 $cm^3 mol^{-1} K$ (**3**)) are slightly higher than the spin-only value, 1.13 $cm^3 mol^{-1} K$, based on a Cu^{II}_3 unit with $S = {}^1/_2$ and assuming $g = 2$, suggesting higher values of g as is usual for Cu^{II} ions. As the temperature is lowered, the $\chi_M T$ versus T curves increase continuously and reach a maximum at 5, 24, and 7 K of 1.78, 1.20, and 1.60 $cm^3 mol^{-1} K$ for complexes **1**, **2**, and **3** respectively, confirming an intramolecular ferromagnetic interaction in the three complexes. On further cooling $\chi_M T$ values decrease abruptly to 1.73, 0.95, and 1.42 $cm^3 mol^{-1} K$ at 1.8 K due to the Zeeman effects, zero-field splitting (zfs) on the Cu^{II}_3 unit, and intercluster antiferromagnetic interactions.

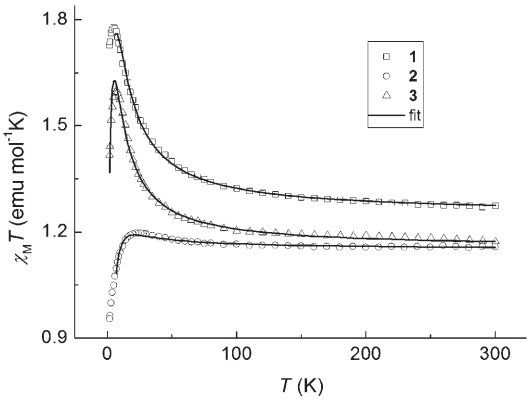

Figure 3. Temperature dependence of the susceptibilities in the form of $\chi_M T$ vs T for complexes **1**–**3**. The solid lines are the fittings in the range between 300 to 5 K for **1**, to 7 K for **2**, and to 1.8 K for **3** (see text).

To quantify the nature of the individual exchange interactions, we noted that the three Cu^{II} ions of each $[Cu_3O_4]$ system occupy alternate partial cube corners. Thus, there are three Cu^{II} ion pairs interacting in each complex with two different exchange pathways for each pair: one involves the μ_3-hydroxo group and the other a bridging keto group of one peripheral 1-benzoylacetone-derived Schiff base. All the Cu^{II} ions are in a distorted square-base pyramid environment with axial bond lengths greater than 2.3 Å, significantly longer than equatorial bonds. Since these axial bonds take part in the keto-mediated exchange pathway between copper ions, we can expect the interactions through the triply bridging hydroxo ligands to be much stronger than the carbonyl ones.[12] For this reason, as a first approximation we will consider only one magnetic exchange constant J between two Cu^{II} ions to avoid overparametrization in the fit. Moreover, since the three copper atoms of the $[Cu_3O_4]$ unit define a quasi-equilateral triangle, we will consider the three metal ions as equivalent, and thus the three magnetic exchange constants of each $[Cu_3O_4]$ core will have the same values. An isotropic Heisenberg–Dirac–van Vleck (HDVV) Hamiltonian formalism for an equilateral triangle [Eq. (1)] was used to estimate the magnitude of the magnetic exchange constant J between Cu^{II} ions.

$$\hat{H} = -2J(\hat{S}_1\hat{S}_2 + \hat{S}_1\hat{S}_3 + \hat{S}_2\hat{S}_3) \quad (1)$$

The magnetic susceptibility deduced from the Hamiltonian is given in Equation (2), in which N, g, β, and k have their usual meanings. When the intercluster interaction is taken into account, the van Vleck equation can be written as in Equation (3).

$$\chi_{trimer} = \frac{Ng^2\beta^2}{4kT} \times \frac{(5\,e^{3J/kT} + 1)}{(e^{3J/kT} + 1)} \quad (2)$$

$$\chi_M = \frac{\chi_{trimer}}{1 - (2zj'/Ng^2\beta^2)\chi_{trimer}} \quad (3)$$

Experimental data for **1**, **2**, and **3**, corrected for diamagnetic contributions and temperature independent paramagnetism (TIP) (0.3×10^{-3} $cm^3 mol^{-1}$), were analyzed by Equation (3) on $\chi_M T$. The best-fit parameters obtained are: $g = 2.108(1)$, $J = 4.49(5)$ cm^{-1}, $zj' = -0.258(5)$ cm^{-1}, $R = 4 \times 10^{-5}$ for complex **1**; $g = 2.023(1)$, $J = 2.95(6)$ cm^{-1}, $zj' = -1.26(1)$ cm^{-1}, $R = 2 \times 10^{-5}$ for complex **2**; $g = 2.026(3)$, $J = 3.58(9)$ cm^{-1}, $zj' = -0.203(5)6$ cm^{-1}, $R = 27 \times 10^{-5}$ for complex **3**, for which R is the agreement factor defined in Equation (4).

$$R = \frac{\sum[(\chi_M T)_{calcd} - (\chi_M T)_{obs}]^2}{\sum(\chi_M T)^{obs}_2} \quad (4)$$

The g values obtained through the fitting procedures are in agreement with other values previously published for $[Cu_3O_4]$ compounds.[3,5] These results confirm the weak ferromagnetic exchange interaction between Cu^{II} ions in all three complexes as well as the antiferromagnetic character of the interactions between trimers. The curves derived from the fits are plotted in Figure 3.

From the field-dependent magnetization values at 1.8 K for the three complexes (Figure 4), the molar magnetization for complex **1** shows a saturation value of $M_s = 2.93\,N\beta\,mol^{-1}$ at 7 T, which provides more evidence of the ferromagnetic coupling between Cu^{II} ions giving rise to a ground state with spin ${}^3/_2$. Complexes **2** and **3** do not reach saturation values at this temperature and at 7 T, probably because of their weaker ferromagnetic exchange interaction and/or the presence of stronger antiferromagnetic intermolecular interactions in the case of **2**.

Temperature-dependent AC magnetic measurements were performed for the three complexes to detect the presence of magnetic ordering. Only **3** showed a nonzero out-of-phase signal (Figure 5). Both real (m') and imaginary (m'') mag-

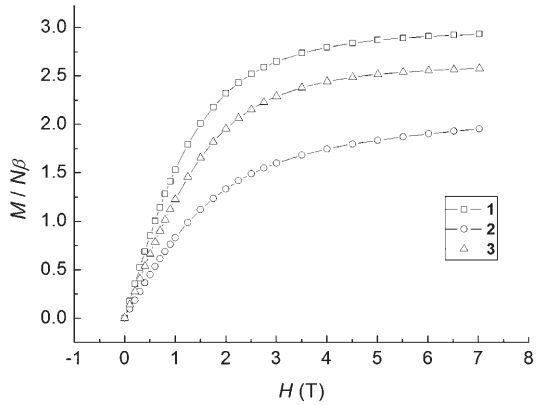

Figure 4. Field dependence of the magnetization for complexes **1**–**3**.

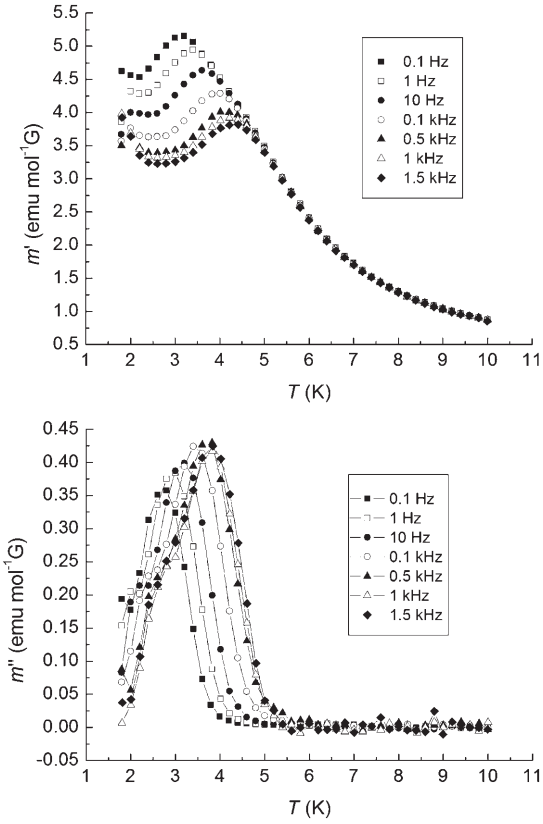

Figure 5. Temperature and frequency dependence of AC magnetization for complex **3**.

netizations show two different frequency-dependent maxima that could be indicative of magnetic transitions. However, no divergence between field-cooled (FC) and Zreo-field-cooled (ZFC) curves at 50 G was observed and further measurements of magnetization at 2 K did not show any hysteresis for this compound, indicating that its blocking temperature is below 2 K. It is important that the higher temperature maxima of the AC measurement for complex **3** shift to higher temperatures with increasing frequencies. At the maximum of the m'' versus T data, the AC angular frequency ω equals the magnetization relaxation rate $1/\tau$. Complex **3** can be characterized in terms of the attempt time τ_0 and the effective energy barrier ΔE necessary for the magnetization relaxation, by analysis of the temperature and frequency dependence of the maxima of the out-of-phase component of the AC susceptibility by a least-squares fit to the Arrhénius law of Equation (5), where $\omega = 2\pi\nu$ is the frequency of the AC applied magnetic field, k_B is the Boltzmann constant, and T is the temperature corresponding to the maximum in the out-of-phase signal.[13]

$$\omega = \frac{1}{\tau_0}\exp\left(\frac{\Delta E}{k_B T}\right) \tag{5}$$

Equation (5) can be transformed into Equation (6), where $1/T$ shows a linear relationship with $\ln(2\pi\nu)$.

$$\frac{1}{T} = -\frac{K_B}{\Delta E}\ln\tau_0 - \frac{k_B}{\Delta}\ln(2\pi\nu) \tag{6}$$

The best fit for the experimental variation of $1/T$ with ν (Figure 6) gives a relaxation time $\tau_0 = 8.1\times10^{-15}$ s and an

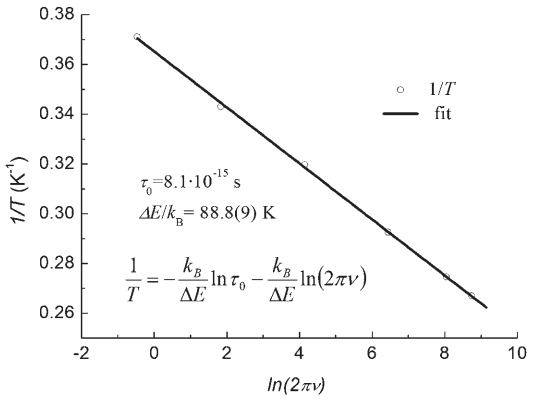

Figure 6. The solid line represents the least-squares fit of the experimental data of $1/T$ versus $\ln(2\pi\nu)$ for the different frequencies applied and maxima observed in the out-of-phase signal of the AC measurement for complex **3**, according to the Arrhénius Equation (4).

energy barrier of $\Delta E/k_B = 88.8(9)$ K (61.6 cm^{-1}). In single-molecule magnets (SMMs) the theoretical energy barrier (Δ) depends only on the magnetic anisotropy of the molecule itself, without any other contribution from the intermolecular three-dimensional network, and can be estimated from $\Delta = |D|S_T^2$ for integer spins or $\Delta = |D|(S_T^2 - {}^1/_4)$ for half-integer spins. In our case, the molecular axial anisotropy parameter D would be unreasonably high to give rise to such an energy barrier, since complex **3** shows a low-spin value of the ground state, $S_T = {}^3/_2$. Even assuming that $D = -1$ cm^{-1}, which is greater in absolute value than for typical Mn_x clusters, would still give a barrier of only 2 cm^{-1}. In the plot of the reduced magnetization ($M/N\mu_B$ versus H/T) for complex **3** (Figure 7), the isofield lines are completely superimposed in the temperature range studied (1.8–10 K), indicating the absence of zero-field splitting (D) in the ground

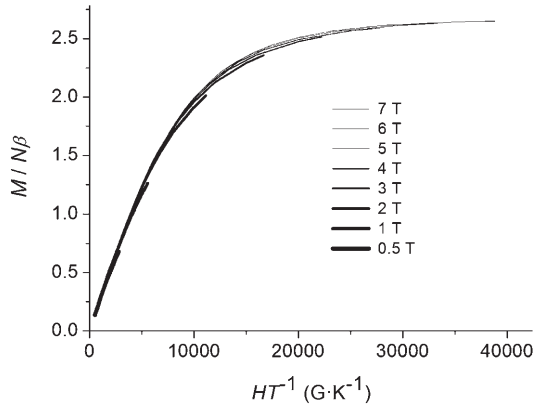

Figure 7. Variation of reduced magnetization (M/$N\beta$ versus H/T) in the range 1.8–10 K for complex **3**.

state of the molecule[14] and thus confirming the non-SMM behavior of this complex.

If the frequency dependence of the positions of the maxima in the AC measurements could be attributed to a long-range three-dimensional magnetic order, the out-of-phase signal would not depend (as it does) on the applied frequency. Further studies must be done to understand the origin of the slow relaxation and determine whether this magnetic transition belongs to a spin–glass freezing process.

Computational details: A detailed description of the computational strategy used to calculate the exchange coupling constants in polynuclear complexes is outside the scope of this paper, but more details can be found in our previous series of papers devoted to such purposes.[12,15,16] We will focus our discussion here on its most relevant aspects. The spin Hamiltonian for a general polynuclear complex without anisotropic terms can be expressed as Equation (7), in which $\hat{S}_i$ and $\hat{S}_j$ are the spin operators of the paramagnetic centers i and j.

$$\hat{H} = -\sum_{i>j} 2J_{ij}\hat{S}_i\hat{S}_j \qquad (7)$$

The J_{ij} parameters are the exchange coupling constants for the different pairwise interactions between the paramagnetic centers of the molecule.

At a practical level, for the evaluation of the n different coupling constants J_{ij} present in a polynuclear complex, we need to carry out calculations for at least $(n+1)$ different spin distributions. Thus, by solving the system of n equations obtained from the energy differences we can obtain the n coupling constants. Where more than n spin distributions were calculated, a fitting procedure was necessary to obtain the coupling constants.[17] In the specific case of the $[Cu_3O_4]$ complexes studied, calculation of the high-spin solution ($S=$ $^3/_2$) and the three $S=^1/_2$ spin distributions corresponding to the inversion of one of the spins allows the three exchange coupling constants to be calculated assuming that the system has no symmetry.

In previous papers, we have analyzed the effect of the basis set and the choice of the functional on the accuracy of the determination of the exchange coupling constants.[12,18] Thus, we found that the hybrid B3LYP functional,[19] together with the basis sets proposed by Schaefer et al., provide J values in excellent agreement with the experimental ones. We have employed a basis set of triple-ζ quality proposed by Schaefer et al.[20] The calculations were performed with the Gaussian 03 code[21] using guess functions generated with the Jaguar 6.0 code.[22]

Continuous shape measurements are described briefly in this section; there is more detailed information on this stereochemical tool and its applications to transition metal compounds in a recent review.[23] The technique was proposed by Avnir and coworkers to provide a quantitative evaluation of the degree of distortion of a set of atoms (for example, the coordination sphere of a transition metal) from a given ideal polyhedral shape.[24,25] In short, the proposed method consists in finding the ideal structure with the desired shape that is closest to the observed structure. The ideal and real polyhedra are superimposed so as to minimize the expression in Equation (8), the value of which is the shape measurement of the structure Q being investigated relative to the ideal shape P, in which $\vec{q}_i$ are N vectors which contain the $3N$ Cartesian coordinates of the problem structure Q, $\vec{p}_i$ contain the coordinates of the ideal polyhedron P, and $\vec{q}_0$ is the position vector of the geometric center which is chosen to be the same for the two polyhedra.

$$S(\mathrm{Q,\ P}) = \min\left[\frac{\sum_{i=1}^{N} |\vec{q}_i - \vec{p}_i|^2}{\sum_{i=1}^{N} |\vec{q}_i - \vec{q}_0|^2}\right] \times 100 \qquad (8)$$

$S(\mathrm{Q,P})=0$ corresponds to a structure Q fully coincident in shape with the reference polyhedron P, regardless of size and orientation. The maximum allowed value is $S(\mathrm{Q,P})=$ 100, although in practice the values found for severely distorted chemical structures are very rarely greater than 40. This method can be employed to analyze the coordination of thousands of structures, as it has been for the ML_4 complexes.[26] Shape measurements were calculated with the SHAPE program.[27]

Discussion

The literature shows some examples of molecular structures with a common $[Cu_3O_4]$ core. Most of the compounds already reported contain acetylacetone-derived Schiff bases as peripheral bridges in their structure. In our effort to increase the number of species belonging to the $[Cu_3O_4]$ family of compounds, we reported the synthesis and magnetic study

of two new triangular compounds using Schiff base ligands prepared by the condensation of different diamines with 1-benzoylacetone.[7] Our aim in this work is to confirm the validity of the previously established magnetostructural correlations for this type of 1-benzoylacetone-derived $[Cu_3O_4]$ compounds also. Therefore we have prepared and characterized structurally and magnetically three more compounds using 1-benzoylacetone-derived Schiff bases. Below, we will first compare the magnitude of the magnetic exchange constants obtained from the fitting procedures for $[Cu_3O_4]$ complexes with analogous or quasi-analogous peripheral bridges, to predict their magnetostructural trends. Then, calculations based on theoretical models and continuous shape measurements (CShMs) will be presented as a helpful tool for studying new magnetostructural correlations for these compounds. Lastly we will examine the rest of the $[Cu_3O_4]$ complexes(**4**–**6**) with other types of Schiff bases to evaluate, again by means of calculations and CShM, the relative effects of the electronic and structural factors relating to the nature of the ligands on the magnitude of the magnetic exchange .

In Table 5 we correlate the values of the J constants with some key structural features for compounds which contain 1-benzoylacetone-derived Schiff bases such as those described in this work (**1**–**3**) and those we reported previously (**4**, **5**)[7] arranged by decreasing value of magnetic exchange constant (J). In Table 5 another $[Cu_3O_4]$ complex (**6**) is included, which was reported by Bian et al. and contains a peripheral bridge derived from the salicylaldehyde instead of the 1-benzoylacetone.[5] Although the two types of ligands in **4**–**6** are different, they both include an aromatic ring in their skeleton, and thus these complexes differ from the rest of the $[Cu_3O_4]$ compounds reported to date. For greater clarity, the structures of the peripheral ligands used in the synthesis of these six compounds have been drawn in Scheme 1. The general trends observed between the six complexes seem to agree with the already well-established magnetostructural correlations for this kind of compound: the further the O(H) group above the plane formed by the three Cu^{II} ions in the triangular complex, the more ferromagnetic the exchange; in the same way, the smaller the Cu-O(H)-Cu′ angle, the more ferromagnetic the magnetic interaction. The coplanarity between the three copper coordination planes (equatorial positions) is also believed to play an important role in the magnitude and nature of the interaction. In these cases, however, this factor is almost constant, since the angles vary in the range of only 79°–82° and no conclusion can be drawn from it. It is important that, while the two previously reported 1-benzoylacetone-derived compounds show an antiferromagnetic interaction, the structural features of those described in this work lead for the first time to ferromagnetically coupled $[Cu_3O_4]$ systems with 1-benzoylacetone-derived Schiff base ligands. This observation encouraged us to perform calculations based on theoretical models and continuous shape measurements to achieve a better understanding of these systems.

Although only one exchange coupling constant has been considered in the fitting of the magnetic susceptibility data for each $[Cu_3O_4]$ complex, for these calculations we have considered an absence of symmetry in these systems. Thus, we have calculated three different exchange coupling constants for each complex and the average values (see Computational details and Table 6). The calculations confirm the ferromagnetic nature of the interactions through the hydroxo/keto bridging ligands, with the exception of a very small antiferromagnetic coupling for the complex **2**. It should be kept in mind that the coupling occurs essentially through the hydroxo ligand because the keto bridging Cu–O bond lengths are rather long due to the Jahn–Teller effect. Hence, the magnetostructural correlations should be sought for the structural parameters of the hydroxo bridging ligand. It is known that for the dinuclear double hydroxo-bridged Cu^{II} complexes,[28,29] the

Table 5. Selected structural parameters for complexes **1**–**6**[a] related to their magnetic properties.

	6	**1**	**3**	**2**	**4**[b]	**5**
Cu1-O(H)-Cu2 [°]	100.2(2)	107.4(1)	103.1(1)	104.6(1)	107.6	107.6(3)
Cu2-O(H)-Cu3 [°]	101.4(2)	105.1(1)	103.1(1)	104.1(1)	106.6	108.1(3)
Cu1-O(H)-Cu3 [°]	102.6(2)	105.3(1)	104.9(1)	105.5(1)	106.9	108.0(3)
Cu-O(H)-Cu′ [°] (av)	101.4	105.9	103.7	104.7	107.0	107.9
O(H)–Cu_3 plane [Å] (av)[c]	0.933	0.774	0.852	0.813	0.751	0.727
Cu/Cu′ [°] (av)[d]	96.6	79.8	81.3	81.6	79.5	81.8
J [cm^{-1}]	7.83	4.49	3.58	2.95	−11.2	−25.6
Ref.	[5]	this work	this work	this work	[7]	[7]

[a] Compounds in the table are in order of decreasing magnetic exchange constant (J). [b] Average values between two nonequivalent molecular entities in the crystal are reported. [c] Deviation of the oxygen atom of the triply bridging hydroxyl group above the plane of the three copper atoms. [d] Coplanarity between the least-squares planes defined by the [O(H),N,N,O] atoms around each Cu^{II} ion; average value calculated from the Cu1/Cu2, Cu2/Cu3, and Cu1/Cu3 dihedral angles.

Table 6. Calculated exchange coupling constants J_{B3LYP} for $[Cu_3O_4]$ complexes (**1**–**3**) indicating the main structural parameters of the exchange pathway and the average values $\bar{J}_{B3LYP}$ for each complex, with the experimental values J_{exp} for comparison.

	Cu-O(H)-Cu′ [°]	d(Cu···Cu) [Å]	J_{B3LYP} [cm^{-1}]	$\bar{J}_{B3LYP}$ [cm^{-1}]	J_{exp} [cm^{-1}]
complex **1**					
J_{12}	105.1	3.187	+6.3	+3.8	+4.49
J_{23}	105.4	3.173	+2.9		
J_{13}	107.4	3.202	+2.3		
complex **2**					
J_{12}	104.5	3.178	–0.8	+4.1	+2.95
J_{23}	104.1	3.175	+8.7		
J_{13}	105.5	3.195	+4.4		
complex **3**					
J_{12}	103.1	3.189	+6.1	+6.0	+3.58
J_{23}	104.9	3.229	+7.7		
J_{13}	103.1	3.185	+4.4		

Cu-O(H)-Cu′ angle together with the out-of-plane shift of the hydrogen atoms modulates the sign and strength of the exchange interaction. This correlation predicts ferromagnetic couplings for large out-of-plane shifts of the hydrogen atoms and small Cu-O(H)-Cu′ angles. Experimentally (Table 5), for the $[Cu_3O_4]$ complexes studied there is a fair correlation between the fitted J values and the Cu-O(H)-Cu′ angle, with some deviations (for instance, the values for complexes **1** and **3**). However, while for the average calculated J values ($\bar{J}_{B3LYP}$) there is a correlation with the Cu-O(H)-Cu′ angle (see Table 6), analysis of the dependence of the nine calculated J values for the three complexes does not show any correlation between the Cu-O(H)-Cu′ bond angles and the exchange coupling constants (see Figure S5).

The analysis of the Cu–O distances and Cu-O(H)-Cu′ angles reveals that some cases with very similar geometrical parameters, for instance J_{12} and J_{23} interactions of the complex **2**, show very different J values, -0.8 and $+8.7$ cm^{-1}, respectively. To explain the results obtained, we have analyzed the coordination sphere of the copper atoms. The Cu^{II} cations adopt a square-pyramid 4+1 coordination very common in Cu^{II} complexes, but with an important distortion of the square-planar moiety. Hence, we should expect a decrease in overlap of the $d_{x^2-y^2}$ orbitals for highly distorted geometries of square-planar Cu^{II} cations, giving rise to a smaller antiferromagnetic contribution and resulting in a larger ferromagnetic coupling. Hence, we have employed continuous shape measurements to analyze how close the four atoms with the shortest Cu–X bond lengths are to an ideal square-planar geometry (see Computational details). In the results (Table S1); the calculated shape measurement S would be zero for an ideal square-planar coordination while a higher number indicates a greater geometrical distortion. To build up a correlation of this parameter with the calculated J_{ij} values, we have represented such values by the product of the S values for the two interacting copper atoms in Figure 8. The correlation is far from perfect, but it shows an interesting dependence between the two magnitudes, especially in the explanation of the antiferromagnetic interaction present in complex **2**. Thus, such antiferromagnetic coupling appears with the two Cu^{II} cations closer to an ideal square-planar coordination and, consequently, with a better overlap between the orbitals bearing the unpaired electrons. A multilinear correlation of the nine calculated J_{ij} values with Cu–O distances, Cu-O(H)-Cu′ bond angles, and the product of the S values indicates that only this last magnitude correlates reasonably with the exchange magnetic constants and that several other structural parameters could play a minor role, but become important when all of them are considered. To verify that this correlation with the coordination sphere of the Cu^{II} cations holds good for similar complexes previously reported (**4**–**6**; see Table 5), we have calculated the shape measurements for such complexes (see Table S1). These values confirm the validity of such a correlation because the complex **6**, showing the strongest ferromagnetic coupling (see Table 5), also presents the largest geometrical distortions from the square-planar coordination, whereas **4** and **5**, with antiferromagnetic couplings, have the copper atoms closest of all the complexes considered to the ideal square-planar coordination.

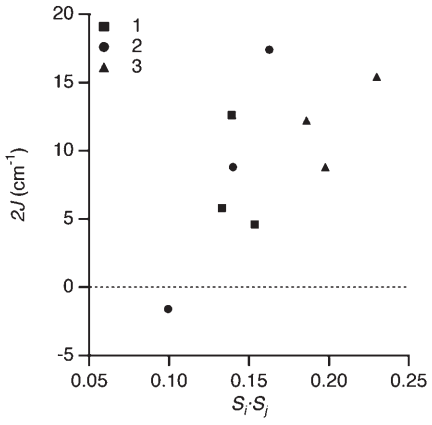

Figure 8. Representation of the variation of the calculated exchange coupling constants (J_{ij}) for the $[Cu_3O_4]$ complexes **1**–**3** by the product of the shape measurement S with respect to the square-planar coordination for the two Cu^{II} cations involved in the exchange interaction.

In Figure 9 we have analyzed the agreement of the calculated J_{ij} values with the experimental data obtained from magnetic susceptibility measurements for **2** without the terms corresponding to the intermolecular interactions. The curve obtained from the calculated J_{ij} values (see Table 6) shows a good agreement with the experimental one, while that corresponding to the average value of the three calculated J_{ij} values shows larger deviations. The results for the other two complexes are similar, confirming that the methodology employed reproduces correctly the physics of the exchange interaction present in the complexes studied.

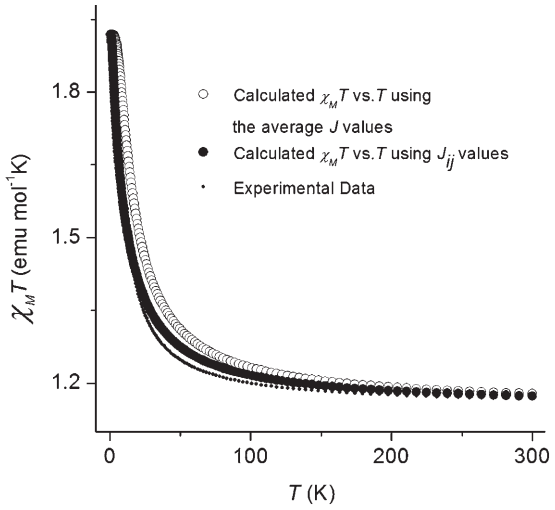

Figure 9. $\chi_M T$ product for the complex **2**: the broken line corresponds to the experimental data without the contribution corresponding to the intermolecular interactions (see Table 6).

Finally, we have analyzed the distribution of the spin density of the ground state $S=3/2$ in complex **2** (Figure 10). The spin density is mostly localized on the Cu^{II} cations. Significant spin delocalization toward donor atoms is associated with the σ-antibonding $d_{x^2-y^2}$ orbitals bearing the unpaired electron.[30,31] The plot reflects clearly the main role of the hydroxo bridging ligand; while the spin delocalization toward the keto bridging ligand is negligible due to the length of the Cu–O bond.

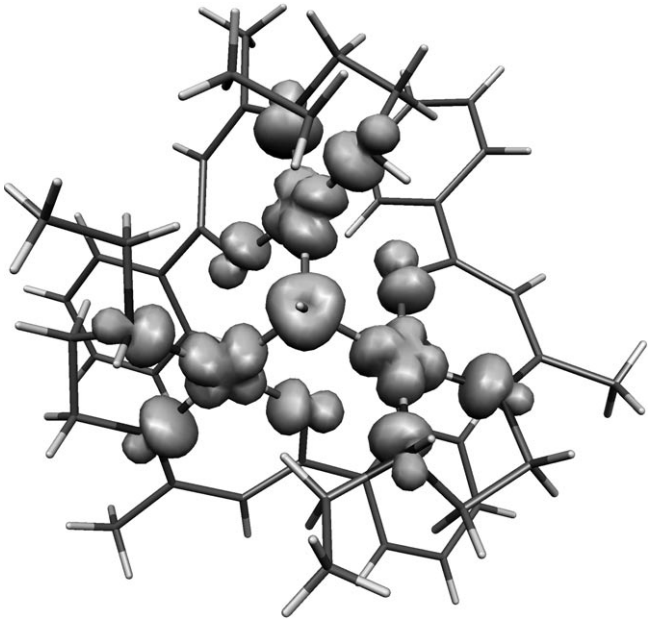

Figure 10. Representation of the spin density map for the ground state of the complex **2**. The isodensity surface represented corresponds to a value of 0.005 e^- $bohr^3$. Clear regions indicate positive spin populations, while negative values are under the threshold employed.

Some anomalies can be detected among the structural factors corresponding to those in Table 5 for some other $[Cu_3O_4]$-type compounds in which aliphatic Schiff bases derived from acetylacetone (**a**–**g**) have been used, when compared with the values discussed for the complexes containing aromatic rings. In Table 7 structural parameters for these compounds have been arranged in decreasing order of magnetic exchange constant, from the most ferro- to the most antiferromagnetic one. Similar values of the two main structural factors studied previously (Cu-O(H)-Cu′; O(H)–Cu_3 plane) provide more antiferromagnetic interaction for the completely aliphatic Schiff base compounds than for the aromatic ones: for example, the Cu-O(H)-Cu′ angles between 103° and 105° seem to lead to ferromagnetic coupling in complexes **2** and **3**, while the coupling turns clearly to antiferromagnetic in complexes **d** and **e**. These data allow us to consider the relative importance of the steric and electronic influences on the magnitude of the magnetic exchange coupling. It appears necessary to check whether increasing aromaticity in bridging ligands could enhance the ferromagnetic character of the magnetic interaction in $[Cu_3O_4]$ compounds, even when the aromatic ring is not directly involved in the bridge. The only $[Cu_3O_4]$ example available where the aromatic ring is situated strictly in the magnetic exchange pathway (complex **6**) shows the strongest ferromagnetic *J* constant. This fact could indicate the importance of the electronic factors.

To confirm or discard the influence of the electronic structure of the ligand in the exchange interaction of $[Cu_3O_4]$ complexes, continuous shape measurements were made for some aliphatic examples from Table 7 to investigate how far the copper environments of the different structures depart from the ideal square-planar coordination. The results indicate that the environments of the copper atoms in these systems are even more distorted from the regular geometry than those of **1**–**6** (Table 5), and hence that more ferromagnetic interactions should be expected. On the contrary, experimental data show more antiferromagnetic exchange; therefore we can conclude that the previous correlation appears not to be valid for $[Cu_3O_4]$ complexes with peripheral aliphatic ligands and so the magnetic exchange interaction cannot be deduced by means of this structural parameter. In calculations using the same computational methodology for an imaginary $[Cu_3O_4]$ system analogous to complex **3**, but where the aromatic ring had been substituted by a methyl group, similar ferromagnetic values of the three J_{ij} exchange coupling constants were obtained; this result allows us to discard an electronic effect arising from the nature of the 1-benzoylacetone. Now it seems clear that the differences in magnitude of the magnetic interaction between the two kinds of system can be attributed entirely to steric effects, and we can be sure that electronic factors arising from the aromatic substituents of the ligands play a minor role in these magnetic systems, although in previous systems they have been shown to diminish the antiferromagnetic strength.[32]

An extensively studied structural parameter in this kind of complex is the coplanarity between the three least-squares planes defined by the donor

Table 7. Selected structural parameters for $[Cu_3O_4]$-type compounds with aliphatic Schiff bases **a**–**g** related to their magnetic properties.[a]

	a	**b**	**c**	**d**	**e**	**f**	**g**
Cu-O(H)-Cu′ [°] (av)	102.9	105.3	106.7	103.2	104.0	105.3	107.9
O(H)–Cu_3 plane [Å] (av)[b]	0.880	0.803	0.769	0.861	0.836	0.797	0.728
Cu/Cu′ [°] (av)[c]	92.3	90.7	83.7	92.5	94.6	85.8	89.7
J [cm^{-1}]	−2.40	−12	−15	−15	−24	−36	−66
Ref.	[5]	[3]	[4]	[6]	[6]	[6]	[6]

[a] Compounds are in order of decreasing value of magnetic exchange constant *J*. [b] Deviation of the oxygen atom of the triply bridging hydroxyl group above the plane of the three copper atoms. [c] Coplanarity between the least-squares planes defined by the [O(H),N,N,O] atoms around each Cu^{II} ion; average value calculated from the Cu1/Cu2, Cu2/Cu3, and Cu1/Cu3 dihedral angles.

atoms around each Cu^{II} ion. Previous studies seem to indicate that the greater the coplanarity, the more antiferromagnetic the interaction becomes. However, this parameter does not show a clear trend among the examples from Tables 5 and 7, since all of these possess a μ_3-hydroxo bridging ligand and hence show average dihedral angles (Cu/Cu′) varying within a narrow range. Clear structural factors inducing the difference in behavior between aliphatic and aromatic $[Cu_3O_4]$ compounds derived from Schiff bases have not been identified, but the steric effect of the aromatic ring on the global structure of the compound seems not to be negligible.

Conclusion

Three new $[Cu_3O_4]$-type compounds have been synthesized and structurally and magnetically characterized. In this work three different 1-benzoylacetone-derived Schiff bases have been used as peripheral bridging ligands, while for all three complexes a hydroxo ligand acts as a triple bridge bonding the three Cu^{II} ions together in the molecular moiety. The three compounds show a global intramolecular ferromagnetic interaction and seem generally to follow the magnetostructural correlations already well established for analogous systems: the greatest distances of the hydroxo group above the plane formed by the three copper ions and the lowest Cu-O(H)-Cu′ angles provide the most ferromagnetic coupling. Moreover, calculations without symmetry restrictions made it possible to observe the influence of a new structural parameter directly correlated to the magnetic exchange magnitude of the three independent interactions (J_{ij}) between Cu^{II} ions in each aromatic $[Cu_3O_4]$ complex derived from a Schiff base. Continuous shape measurements are a powerful tool for studying the divergence of the metal coordination environments from an ideal geometry. In the $[Cu_3O_4]$ complexes derived from aromatic Schiff bases studied in this work, we found a correlation between the degree of distortion of the square-planar geometry of the Cu^{II} ions and the magnitude of the magnetic interaction: highly distorted geometries led to more ferromagnetic interactions. In our case, the substitution of hydrogen atoms in the terminal amine group of the 1-benzoylacetone-derived Schiff bases by more voluminous groups such as methyl, dimethyl, or ethyl could cause these structural changes in the molecular entity that would consequently decrease the overlap of the magnetic orbitals of the Cu^{II} ions, giving rise to ferromagnetic interactions. This is a new example of the structure-dependent modification of the magnetic properties in molecular compounds. However, continuous shape measurements on similar $[Cu_3O_4]$ compounds derived from aliphatic Schiff bases seem to demonstrate the limits of this correlation: higher geometric distortions than are observed in aromatic-derived compounds still lead to antiferromagnetic exchange interactions. New correlations should be found in order to elucidate the different trend between these two types of compound, but, in any case, theoretical models allow an electronic influence from the nature of the ligands to be excluded; only structural factors should be considered. Magnetic order in complex **3** is deduced from the nonzero out-of-phase signal observed in AC measurements. However, the low-spin value of its ground state ($S = {}^3/_2$) and the negligible zero field splitting (D) in the molecular system indicate that **3** does not belong to the SMM family. The origin of this magnetic order is still unclear.

Experimental Section

Materials: The three monocondensed Schiff base ligands HL^1, HL^2, and HL^3 have been synthesized in our laboratory by the methods described below. The diamines and 1-benzoylacetone were purchased from Lancaster Chemical Co. The chemicals were of reagent grade and used without further purification.

CAUTION! Although no problems were encountered in this work, perchlorate salts containing organic ligands are potentially explosive. They should be prepared in small quantities and handled with care.

Preparation of HL^1, HL^2, and HL^3: HL^1, HL^2, and HL^3 were prepared by condensation of the NH_2 group of *N*-methyl-1,2-ethanediamine (0.74 mL, 10 mmol), *N*-ethyl-1,2-ethanediamine (0.90 mL, 10 mmol), and *N*,*N*-dimethyl-1,2-ethanediamine (0.88 mL, 10 mmol), respectively, with 1-benzoylacetone (1 g, 10 mmol) in methanol (20 mL) under reflux for 2 h. The Schiff base ligands were not isolated and the yellow methanolic solutions were used directly for formation of the complexes.

Synthesis of 1, 2, and 3: The clear solution of $Cu[ClO_4]_2{\cdot}6H_2O$ (3.7 g,10 mmol) in methanol (20 mL) was added to solutions of the tridentate Schiff base ligands HL^1, HL^2, and HL^3 (10 mmol) in methanol (20 mL), and the mixed solution was stirred well. Triethylamine (1.7 mL, 10 mmol) was added dropwise to the resulting solution with constant stirring .The greenish precipitate of complex **1** and bluish-green precipitate of complex **3**, which appeared immediately, were filtered and the filtrate was kept several days in a refrigerator to yield single dark green hexagonal crystals of **1** and single blue cubic crystals of **3**. In the case of **2**, a small amount of green hydrolyzed product which separated immediately during the addition of triethylamine was filtered off; the amount of this hydrolyzed product increased if the methanol contained water. Therefore the methanol was dried before being used as a solvent for the synthesis of **2**. The resulting green filtrate of **2** was set aside at room temperature. Overnight, crystalline product for **2** appeared as green prisms. Single-crystals suitable for X-ray diffraction analysis were obtained by diffusion of *n*-hexane into the solution of **2** in dichloromethane.

*Complex **1***: Yield: 3.0 g (75%); UV/Vis (acetonitrile): $\lambda_{max}(\varepsilon_{max}) = 591$ nm (249 $dm^3 mol^{-1} cm^{-1}$); IR: $\tilde{\nu} = 1515$ (C=N), 3249, 3287 (N–H), 3400, 3510 cm^{-1} (O–H); elemental analysis calcd (%) for $C_{39}H_{58}Cl_2Cu_3N_6O_{15}$ (1112.43): C 42.11, H 5.26, N 7.55, Cu 17.14; found: C 42.32, H 5.36, N 7.57, Cu 17.53.

*Complex **2***: Yield: 2.0 g (60%); UV/Vis (acetonitrile): $\lambda_{max}(\varepsilon_{max}) = 587$ nm (280$dm^3 mol^{-1} cm^{-1}$); IR: $\tilde{\nu} = 1520$ (C=N), 3247, 3270 (N–H), 3440, 3502 cm^{-1} (O–H); elemental analysis calcd (%) for $C_{42}H_{60}Cl_2Cu_3N_6O_{13}$ (1118.48): C 45.10, H 5.41, N 7.51, Cu 17.04; found: C 44.96, H 5.66, N 7.53, Cu 17.34.

*Complex **3***: Yield: 3.5 g (80%); UV/Vis (acetonitrile): $\lambda_{max}(\varepsilon_{max}) = 581$ nm (281$dm^3 mol^{-1} cm^{-1}$); IR: $\tilde{\nu} = 1518$ (C=N), 3450, 3528 cm^{-1}(O–H); elemental analysis calcd (%) for $C_{42}H_{72}Cl_2Cu_3N_6O_{19}$ (1226.59): C 41.13, H 5.92, N 6.85, Cu 15.54; found: C 40.94, H 5.82, N 6.51, Cu 16.06.

Elemental analysis and spectroscopy: Elemental analyses (C, H, N) were performed using a Perkin–Elmer 240C elemental analyzer and the copper contents in all the complexes were estimated spectrophotometrically.[33] IR spectra in KBr (4500–500 cm^{-1}) were recorded using a Perkin–Elmer RXI FT-IR spectrophotometer. Electronic spectra in methanol (1200–350 nm) were recorded in a Hitachi U-3501 spectrophotometer.

X-ray structure determinations: Single-crystal X-ray diffraction measurement for **1**, **2**, and **3** was carried out on a Brucker SMART Apex CCD diffractometer with graphite monochromatized $Mo_{K\alpha}$ radiation ($\lambda =$ 0.71073 Å) using both Φ and ω scan modes at 293 K. Intensity data were collected in the θ range of 2.11–24.55 for complex **1**, 2.03–25.22 for complex **2**, and 2.45–17.81 for complex **3**; data reduction was performed with the Bruker SAINT package.[34] Absorption corrections were made using the SADABS program.[35] The structure was solved by direct methods and refined on F^2 by full-matrix least-squares using SHELXL-97[36] with anisotropic displacement parameters for all non-hydrogen atoms. H atoms were introduced in calculations using the riding model. All computations were carried out using the SHELXTL-2000 program package.[37] Significant crystallographic data are summarized in Table 1. Selected bond lengths and bond angles are gathered in Tables 2 and 3.

CCDC-644822 (**1**), CCDC-644823 (**2**), and CCDC-644824 (**3**) contain the supplementary crystallographic data for this paper. These data can be obtained free of charge from The Cambridge Crystallographic Data Centre via www.ccdc.cam.ac.uk/data_request/cif.

Magnetic measurements: The magnetic measurements were carried out on polycrystalline samples using a Quantum Design SQUID MPMS-XL7 magnetometer in the range 2–300 K at an applied magnetic field of 0.2 T. The diamagnetic corrections were evaluated from Pascal's constants.

Acknowledgements

This work was supported financially by the Spanish Government (grant CTQ2006–03949). The research reported here was also supported by the Dirección General de Investigación del Ministerio de Educación y Ciencia and the Comissió Interdepartamental de Ciència i Tecnologia (CIRIT) through grants CTQ2005–08123-C02–02/BQU and 2005SGR–00036, respectively. The computing resources were generously made available at the Centre de Computació de Catalunya (CESCA) through a grant provided by the Fundació Catalana per a la Recerca (FCR) and the Universitat de Barcelona. We also thank Núria Clos, Unitat de Mesures Magnètiques, Serveis Científics i Tècnics, Universitat de Barcelona, for the magnetic measurements.

[1] a) O. Kahn, *Chem. Phys. Lett.* **1997**, *265*, 165; b) G. Aromi, S. M. J. Aubin, M. A. Bolcar, G. Christou, H. J. Eppley, K. Folting, D. N. Hendrickson, J. C. Huffman, R. C. Squire, H. L. Tsai, S. Wang, M. W. Wemple, *Polyhedron* **1998**, *17*, 3005; c) L. Thomas, F. Lionti, R. Ballou, D. Gatteschi, R. Sessoli, B. Barbara, *Nature* **1996**, *383*, 145; d) K. Wieghart, K. Pohl, H. Jibril, G. Huttner, *Angew. Chem.* **1984**, *96*, 66; *Angew. Chem. Int. Ed. Engl.* **1984**, *23, 77*; e) C. Sangregorio, T. Ohm, C. Paulsen, R. Sessoli, D Gatteschi, *Phys. Rev. Lett.* **1997**, *78*, 4645; for detailed references, see: f) S. M. J. Aubin, Z. Sun, H. J. Eppley, E. M. Rumberger, E. A. Guzei, K. Folting, P. K. Gantzel, A. L. Rheingold, G. Christou, D. N. Hendrickson, *Inorg. Chem.* **2001**, *40*, 2127; g) *Magnetic Molecular Materials* (Eds.: D. Gatteschi, O. Kahn, J. S. Miller, F. Palacio), Kluwer Academic, Dordrecht (The Netherlands), **1991**; h) O. Kahn, Y. Pei, Y. Yournaux, *Inorganic Materials* (Eds.: D. W. Bruce, O. O. Hare), Wiley, Chichester, **1992**; i) O. Kahn, *Molecular Magnetism*, VCH, Weinheim, **1993**; j) "Molecular-Based Magnetic Materials: Theory, Techniques and Applications": *ACS Symp. Ser.* **1996**, *644*, whole volume.

[2] a) V. H. Crawford, H. W. Richardson, J. R. Wasson, D. J. Hodgson, W. E. Hatfield, *Inorg. Chem.* **1976**, *15*, 2107; b) L. K. Thompson, S. K. Mandal, S. S. Tandon, J. N. Bridson, M. K. Park, *Inorg. Chem.* **1996**, *35*, 3117; c) E. Ruiz, P. Alemany, S. Alvarez, J. Cano, *Inorg. Chem.* **1997**, *36*, 3683; d) A. Mukherjee, R. Raghunathan, M. K. Saha, M. Nethaji, S. Ramasesha, A. R. Chakravarty, *Chem. Eur. J.* **2005**, *11*, 3087.

[3] J. P. Costes, F. Dahan, J. P. Laurent, *Inorg. Chem.* **1986**, *25*, 413.

[4] M. Kwiatkowski, E. Kwiatkoski, A. Olechnowicz, D. M. Ho, E. Deutsch, *Inorg. Chim. Acta* **1988**, *150*, 65.

[5] H. D. Bian, J. Y. Xu, W. Gu, S. P. Yan, P. Cheng, D. Z. Liao, Z. H. Jiang, *Polyhedron* **2003**, *22*, 2927.

[6] M. S. Ray, S. Chattopadhyay, M. G. B. Drew, A. Figuerola, J. Ribas, C. Diaz, A. Ghosh, *Eur. J. Inorg. Chem.* **2005**, 4562.

[7] B. Sarkar, M. S. Ray, M. G. Drew, A. Figuerola, C. Diaz, A. Ghosh, *Polyhedron* **2006**, *25*, 3084.

[8] a) B. J. Hathaway, *Comprehensive Coordination Chemistry, Vol. 5*, (Eds: G. Wilkinson, R. D. Gillard, J. A. McCleverty), Pergamon, Oxford, **1987**, p. 533; b) B. J. Hathaway, *Struct. Bonding* **1984**, *57*, 55.

[9] a) J. P. Costes, F. Dahan, J. P. Laurent, *J. Coord. Chem.* **1984**, *13*, 355; b) J. P. Costes, F. Dahan, J. P. Laurent, *Inorg. Chem.* **1985**, *24*, 1018.

[10] A. W. Addison, T. N. Rao, J. Reedjik, J. van Rijn, C. G. Verschoor, *J. Chem. Soc. Dalton Trans.* **1984**, 1349.

[11] a) D. Cremer, J. A. Pople, *J. Am. Chem. Soc.* **1975**, *97*, 1354; b) J. C. A. Boyens, *J. Cryst. Mol. Struct.* **1978**, *8*, 31.

[12] E. Ruiz, S. Alvarez, J. Cano, V. Polo, *J. Chem. Phys.* **2005**, *123*, 164110.

[13] P. Gerbier, N. Domingo, J. Gómez-Segura, D. Ruiz-Molina, D. B. Amabilino, J. Tejada, B. E. Williamson, J. Veciana, *J. Mater. Chem.* **2004**, *14*, 2455–2460.

[14] E. C. Sañudo, W. Wernsdorfer, K. A. Abboud, G. Christou, *Inorg. Chem.* **2004**, *43*, 4137–4144.

[15] E. Ruiz, J. Cano, S. Alvarez, P. Alemany, *J. Comput. Chem.* **1999**, *20*, 1391.

[16] E. Ruiz, A. Rodríguez-Fortea, J. Cano, S. Alvarez, P. Alemany, *J. Comput. Chem.* **2003**, *24*, 982.

[17] E. Ruiz, *Struct. Bonding* **2004**, *113*, 71.

[18] "Electronic structure and magnetic behavior in polynuclear transition-metal compounds": E. Ruiz, S. Alvarez, A. Rodríguez-Fortea, P. Alemany, Y. Pouillon, C. Massobrio in *Magnetism: Molecules to Materials, Vol. 2* (Eds: J. S. Miller, M. Drillon), Wiley-VCH, Weinheim, **2001**, p. 227.

[19] A. D. Becke, *J. Chem. Phys.* **1993**, *98*, 5648.

[20] A. Schaefer, C. Huber, R. Ahlrichs, *J. Chem. Phys.* **1994**, *100*, 5829.

[21] Gaussian 03 (Revision C.01), M. J. Frisch, G. W. Trucks, H. B. Schlegel, G. E. Scuseria, M. A. Robb, J. R. Cheeseman, J. A. Montgomery Jr., T. Vreven, K. N. Kudin, J. C. Burant, J. M. Millam, S. S. Iyengar, J. Tomasi, V. Barone, B. Mennucci, M. Cossi, G. Scalmani, N. Rega, G. A. Petersson, H. Nakatsuji, M. Hada, M. Ehara, K. Toyota, R. Fukuda, J. Hasegawa, M. Ishida, T. Nakajima, Y. Honda, O. Kitao, H. Nakai, M. Klene, X. Li, J. E. Knox, H. P. Hratchian, J. B. Cross, C. Adamo, J. Jaramillo, R. Gomperts, R. E. Stratmann, O. Yazyev, A. J. Austin, R. Cammi, C. Pomelli, J. W. Ochterski, P. Y. Ayala, K. Morokuma, G. A. Voth, P. Salvador, J. J. Dannenberg, V. G. Zakrzewski, S. Dapprich, A. D. Daniels, M. C. Strain, O. Farkas, D. K. Malick, A. D. Rabuck, K. Raghavachari, J. B. Foresman, J. V. Ortiz, Q. Cui, A. G. Baboul, S. Clifford, J. Cioslowski, B. B. Stefanov, G. Liu, A. Liashenko, P. Piskorz, I. Komaromi, R. L. Martin, D. J. Fox, T. Keith, M. A. Al-Laham, C. Y. Peng, A. Nanayakkara, M. Challacombe, P. M. W. Gill, B. Johnson, W. Chen, M. W. Wong, C. Gonzalez, J. A. Pople, Gaussian, Inc., Pittsburgh, PA, **2004**.

[22] Jaguar 6.0, Schrödinger, Inc., Portland, OR, **2005**.

[23] S. Alvarez, P. Alemany, D. Casanova, J. Cirera, M. Llunell, D. Avnir, *Coord. Chem. Rev.* **2005**, *249*, 1693.

[24] D. J. Avnir, O. Katzenelson, S. Keinan, M. Pinsky, Y. Pinto, Y. Salomon, H. Zabrodsky Hel-Or, in *Concepts in Chemistry: A Contemporary Challenge*, Research Studies, Taunton, UK, **1997**.

[25] H. Zabrodsky, S. Peleg, D. J. Avnir, *J. Am. Chem. Soc.* **1992**, *114*, 7843.

[26] J. Cirera, P. Alemany, S. Alvarez, *Chem. Eur. J.* **2004**, *10*, 190.

[27] M. Llunell, D. Casanova, J. Cirera, J. M. Bofill, P. Alemany, S. Alvarez, M. Pinsky, D. Avnir, SHAPE program, Version 1.1, Barcelona, **2003**.

[28] E. Ruiz, P. Alemany, S. Alvarez , J. Cano, *J. Am. Chem. Soc.* **1997**, *119*, 1297.

[29] E. Ruiz, P. Alemany, S. Alvarez, J. Cano, *Inorg. Chem.* **1997**, *36*, 3683.

[30] J. Cano, E. Ruiz, S. Alvarez, M. Verdaguer, *Comments Inorg. Chem.* **1998**, *20*, 27.
[31] E. Ruiz, J. Cirera, S. Alvarez, *Coord. Chem. Rev.* **2005**, *249*, 2649.
[32] a) Md. E. Ali, S. N. Datta, *J. Phys. Chem. A* **2006**, *110*, 2776–2784; b) E. Ruiz, S. Alvarez, P. Alemany, *Chem. Commun.* **1998**, 2767–2768.
[33] G. H. Jeffery, J. Bassett, J. Mendham, R. C. Denney *Vogel's Textbook of Quantitative Chemical Analysis,* 5th ed., Longman Scientific and Technical, New York, **1989**, p. 689.
[34] Bruker SMART and SAINT, version 6.22a, Bruker AXS, Inc., Madison, WI, **1999**.
[35] G. M. Sheldrick, SADBS, version 2, Multi-scan Absorption Correction Program, University of Göttingen, Germany, **2001**.
[36] G. M. Sheldrick, SHELX 97, Programs for Crystal Structure Solution and Refinement, University of Göttingen, Germany, **1997**.
[37] Bruker, SMART, SAINT, SADABS and SHELXTL, Bruker AXS, Inc., Madison, WI, USA, **2000**.

Received: April 25, 2007
Published online: August 31, 2007

